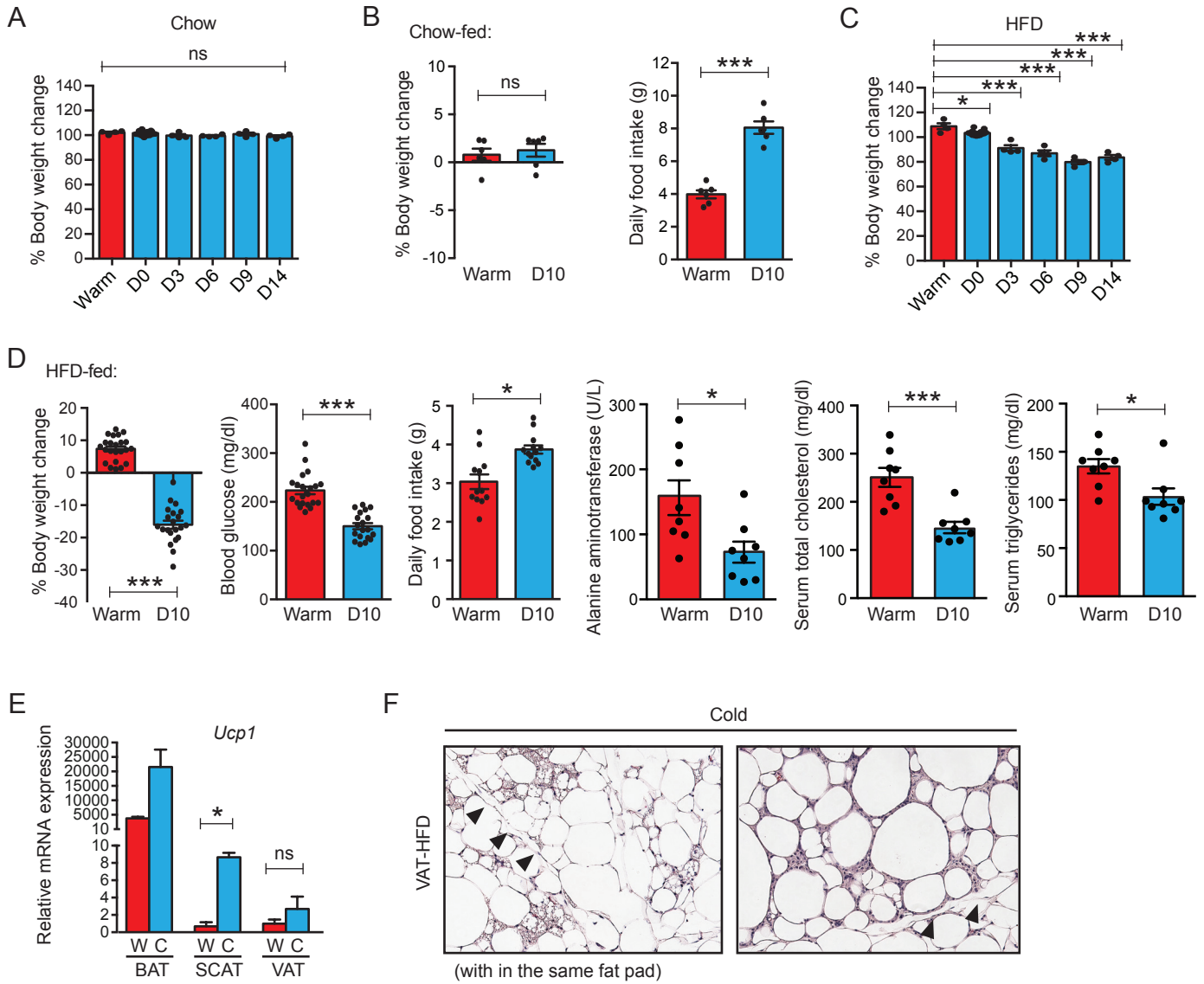


Supplemental Information

Adaptive adipose tissue stromal plasticity in response to cold stress and antibody-based metabolic therapy

Joshua C. Chang, Steffen Durinck, Mark Z. Chen, Nadia Martinez-Martin, Jingli A. Zhang, Isabelle Lehoux, Hong Li, May Lin, Jiansheng Wu, Travis W. Bainbridge, James A. Ernst, Sree R. Ramani, Sairupa Paduchuri, Lance Kates, Margaret Solon, Matthew B. Buechler, Alessandra Castiglioni, Minh Thai, Beatrice Breart, Zora Modrusan, Andrew S. Peterson, Shannon J. Turley, Junichiro Sonoda

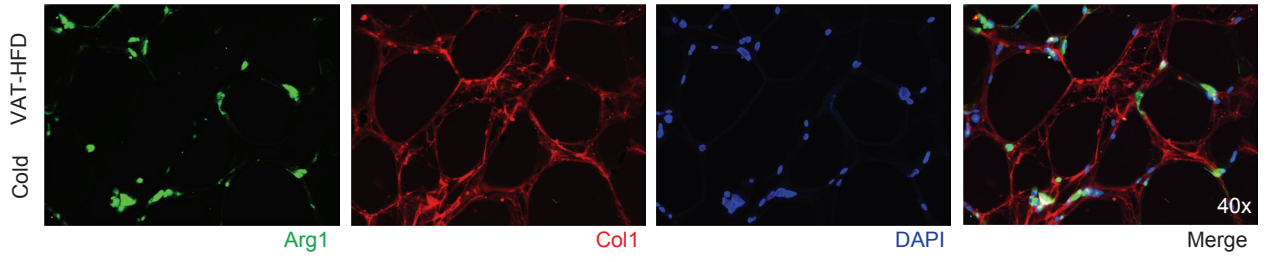
Fig. S1



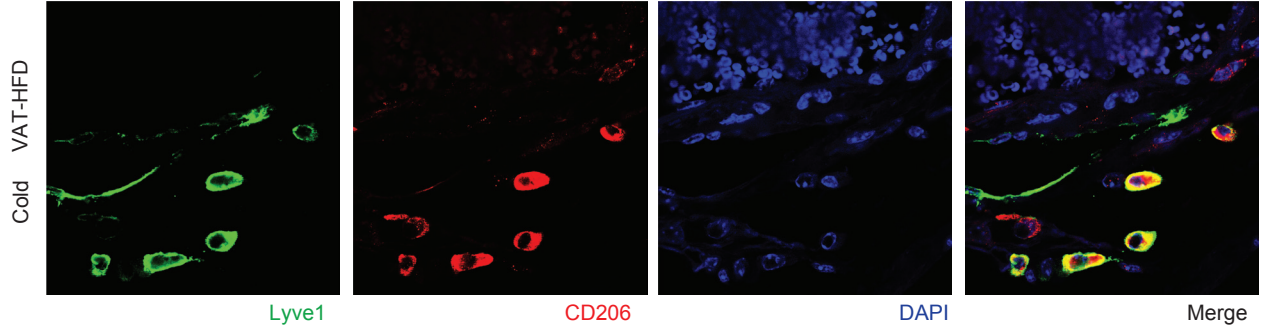
Supplemental Figure S1. Cold exposure induces weight loss and browning in obese mice. C57BL/6 mice on either **(A-B)** normal chow (10% kcal fat) or **(C-F)** HFD (60% kcal fat) were maintained at thermoneutrality (30°C, Warm) or exposed to 4°C (Cold) after adaptation at 18°C. **(A)** Body weight change % (from day -5) after exposed to 4°C cold for the indicated time, or control Warm mice maintained under thermoneutrality until day 14 (red) (N=4 mice per group). The starting body weights were 29.8 ± 0.2 g. **(B)** Body weight changes and food intake of chow-fed mice during 4°C cold exposure for 10 days. (N=6 mice per group). **(C)** Body weight changes % (from day -5) of HFD-fed DIO mice after exposed to 4°C cold for the indicated time, or control Warm mice maintained under thermoneutrality until day 14 (red) (N=4 mice per group). The starting body weights were 46.5 ± 0.7 g. **(D)** Body weight changes, blood glucose (N \geq 18 mice per group), food intake (N=12 mice per group), serum total alanine aminotransferase, cholesterol, and triglycerides (N=8 mice per group) in DIO mice after 4°C cold exposure for 10 days. **(E)** qPCR analysis of *Ucp1* mRNA expression in BAT (N=3), SCAT, and VAT (N=5~6) in cold exposed (10 days) DIO mice. Statistical analysis was conducted without considering BAT samples. **(F)** H&E staining of cold exposed HFD-fed VAT. Both images are from the same fat pad. Triangles indicate fibrous septa. * $P < 0.05$, ** $P < 0.01$, *** $P < 0.001$ by one-way ANOVA (A and C) or by student t-test (B, D and E). Data are shown as mean \pm SEM.

Fig. S2

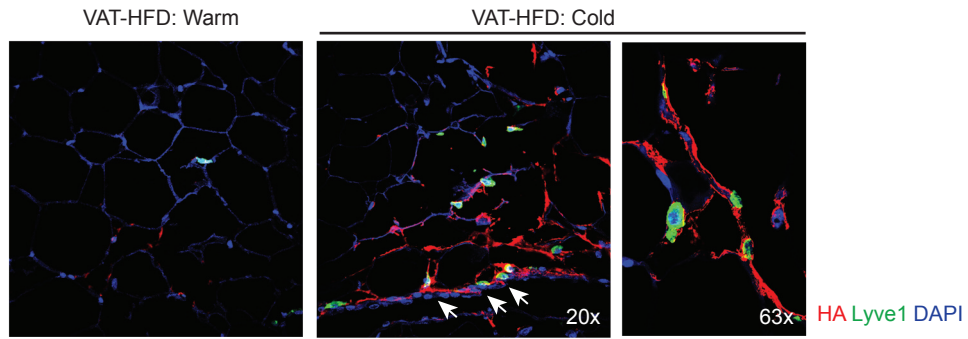
A



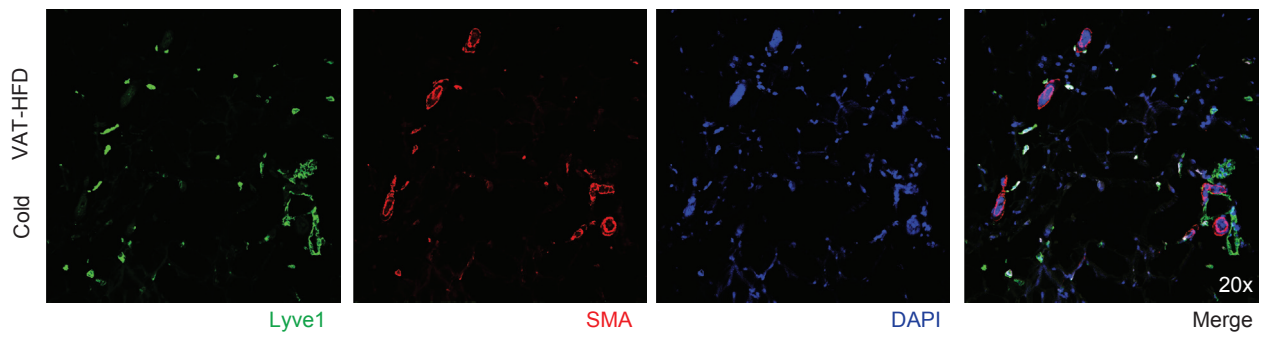
B



C

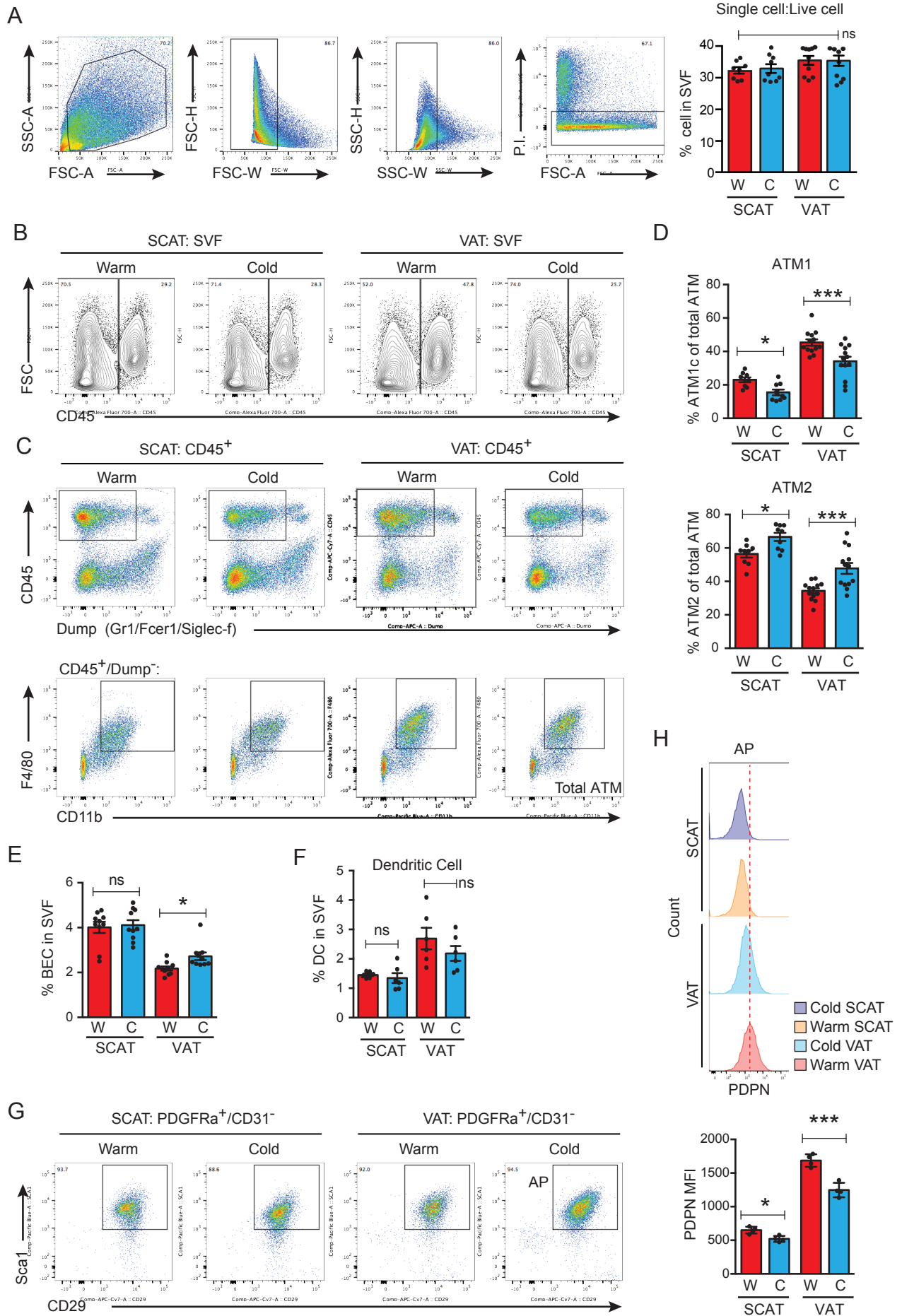


D



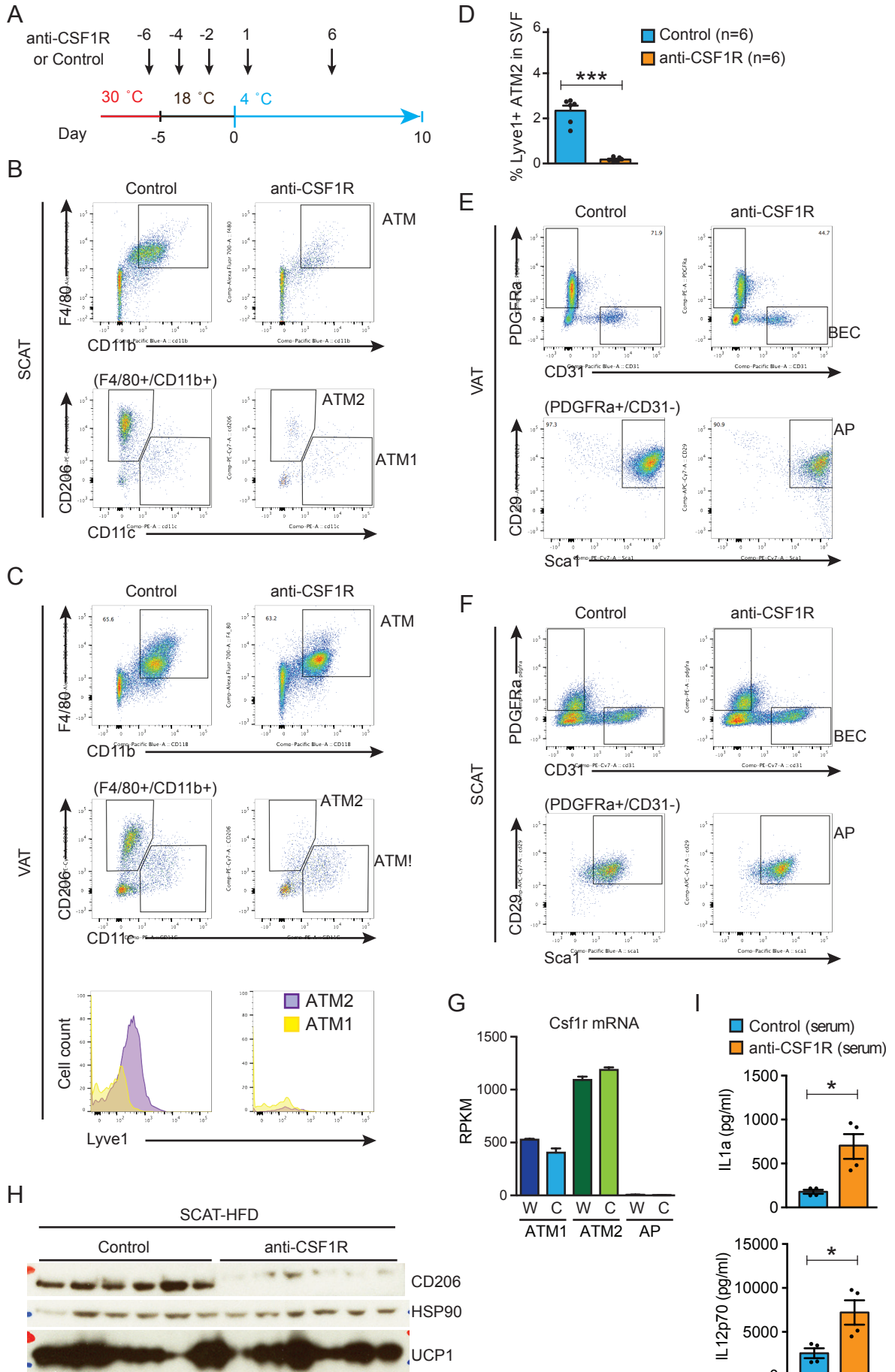
Supplemental Figure S2. Cold exposure induces VAT remodeling in obese mice. HFD-fed mice were maintained at 30°C (Warm) or exposed to 4°C for 10 days (Cold). **(A)** The same images as Figure 2B split into single channels. **(B)** The same images as Figure 2D split into single channels. **(C)** HA (red) and Lyve1 (green) IF. **(D)** The same images as Figure 2F split into single channels. DAPI (blue) stains cell nuclei in all IF.

Fig. S3



Supplemental Figure S3. Cold exposure recruits ATM2. HFD-fed mice were maintained at 30°C (Warm) or exposed to 4°C for 10 days (Cold). Flow cytometry analysis of SVF from both SCAT and VAT are shown. **(A)** The gating strategy of live cells in adipose tissue SVF. Frequencies of live cells in SVF at right. **(B)** Representative flow cytometry plots showing CD45⁺ or CD45⁻ cells in live SVF. **(C)** Representative flow cytometry plots showing CD45⁺/F4/80⁺/CD11b⁺/Dump⁻ ATM in total live SVF. **(D)** Frequencies of CD11c⁺/CD206⁻ ATM1 and CD11c⁻/CD206⁺ ATM2 in total CD45⁺/F4/80⁺/CD11b⁺/Dump⁻ ATM. **(E)** Frequencies of CD31⁺/PDPN⁻/CD45⁻ BEC in total SVF. **(F)** Frequencies of CD45⁺/Dump⁻/F4/80⁻/CD11c⁺ dendritic cells in total SVF. **(G)** Representative flow cytometry plots showing CD45⁻/CD31⁻/PDGFR α ⁺/Sca1⁺/CD29⁺ AP. **(H)** Flow cytometry histogram showing PDPN expression level in AP (left) and the quantification of the PDPN MFI (right). PDPN is an inflammation marker. * $P < 0.05$, ** $P < 0.01$, *** $P < 0.001$ by student t-test. Data are shown as mean \pm SEM.

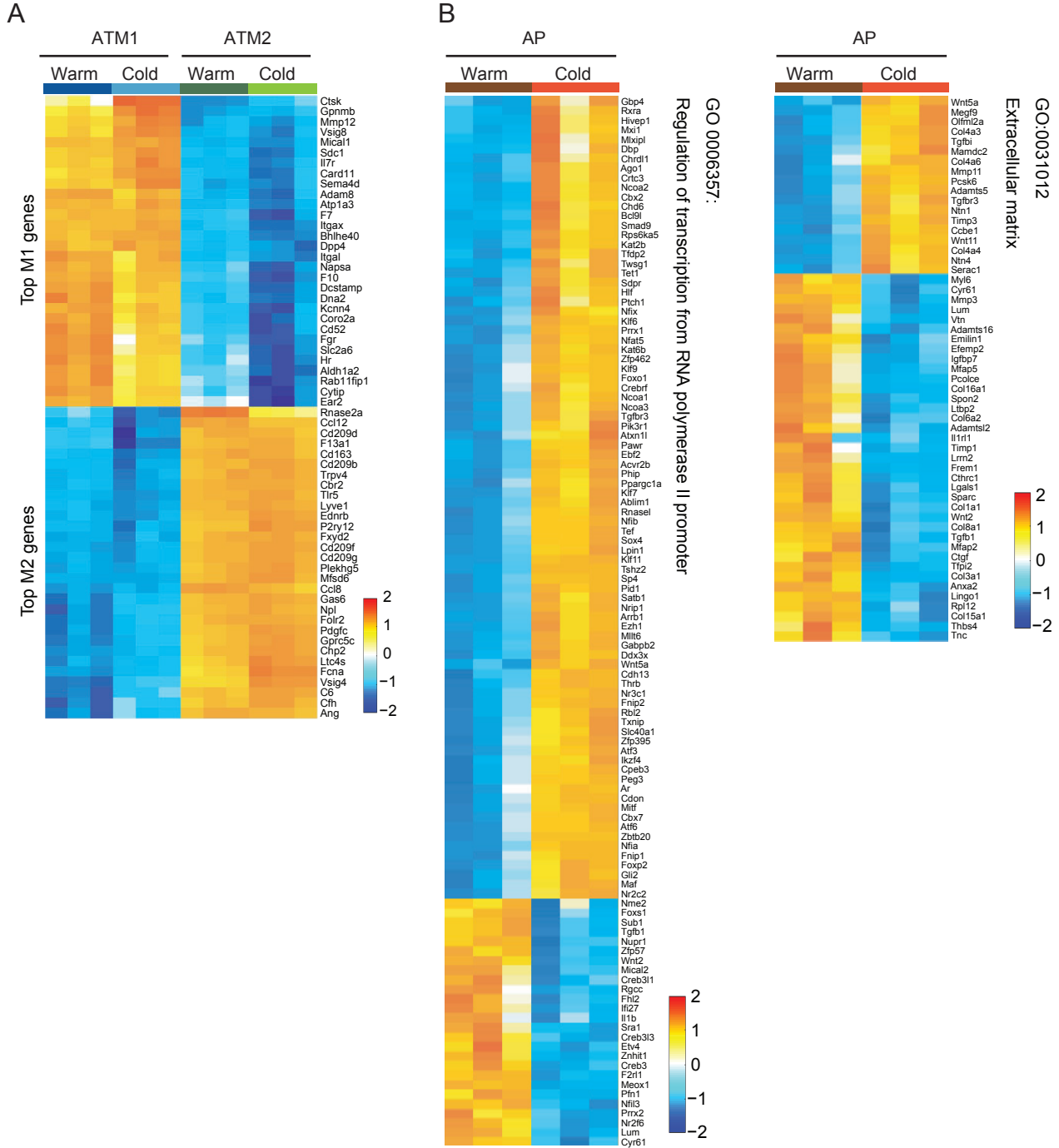
Fig. S4



Supplemental Figure S4. CSF1R signaling is required for cold-induced recruitment of ATM2. (A)

The design for the anti-CSF1R experiment. HFD-fed C57BL/6 male mice maintained at thermoneutrality were i.p. dosed with 40 mg/kg anti-CSF1R antibody or isotype control at indicated times (arrows). All the mice were exposed to 4°C for 10 days after acclimation for 5 days at 18 °C. **(B)** Representative flow cytometry plots showing total ATM (top), ATM1 and ATM2 (bottom) in SCAT with or without anti-CSF1R treatment. **(C)** Representative flow cytometry plots showing total ATM (top), ATM1 and ATM2 (middle), and Lyve1 histograms in ATM1 and ATM2 populations (bottom) in VAT, with or without anti-CSF1R treatment. **(D)** Frequencies of Lyve1⁺ ATM2 in total SVF with or without anti-CSF1R treatment. **(E)** Representative FACS plots showing AP in VAT with or without anti-CSF1R treatment. **(F)** Representative FACS plots showing AP in SCAT with or without anti-CSF1R treatment. **(G)** *Csf1r* mRNA expression in ATM1, ATM2, and AP in warm or cold-exposed VAT by RNA-seq (N=3). **(H)** Western blot analysis for CD206 and UCP1 expression in obese SCAT with or without anti-CSF1R treatment. HSP90 serves as loading control. **(I)** Cytokine concentrations in serum. * $P < 0.05$, *** $P < 0.001$ by student t-test. Data are shown as mean \pm SEM.

Fig. S5

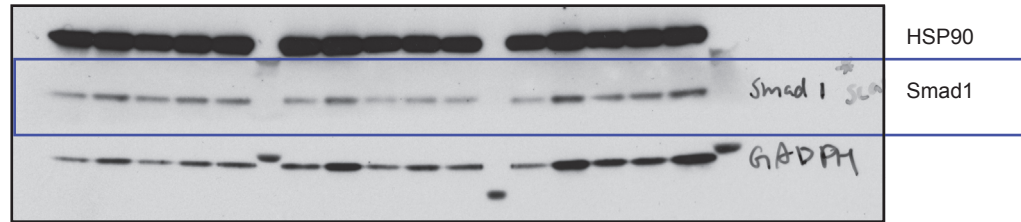


Supplemental Figure S5. Heatmap showing ATM and AP gene expression in warm and cold

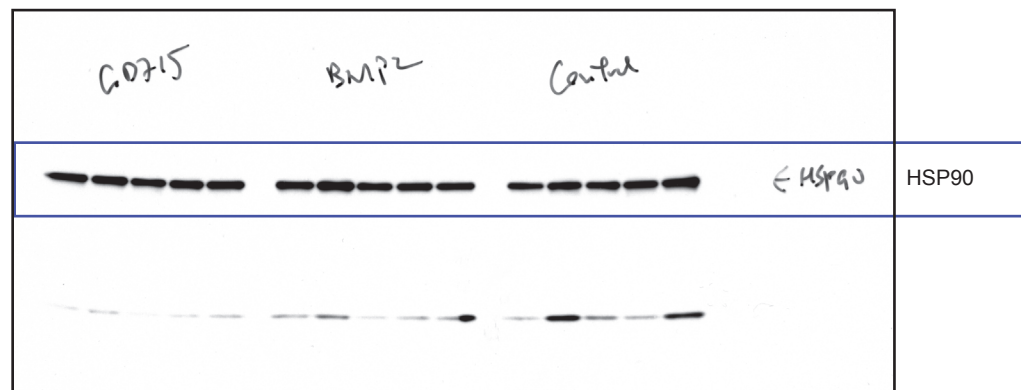
conditions. (A) Heatmap showing top 20 ATM1 and ATM2 gene and their expression in warm and cold conditions. (B) Heatmap showing AP expression of various genes in indicated GO pathways. For heatmaps, expression data ($\log_2(\text{RPKM})$) are standardized along each gene (row), and color scale corresponds to the relative expression level.

Fig. S6

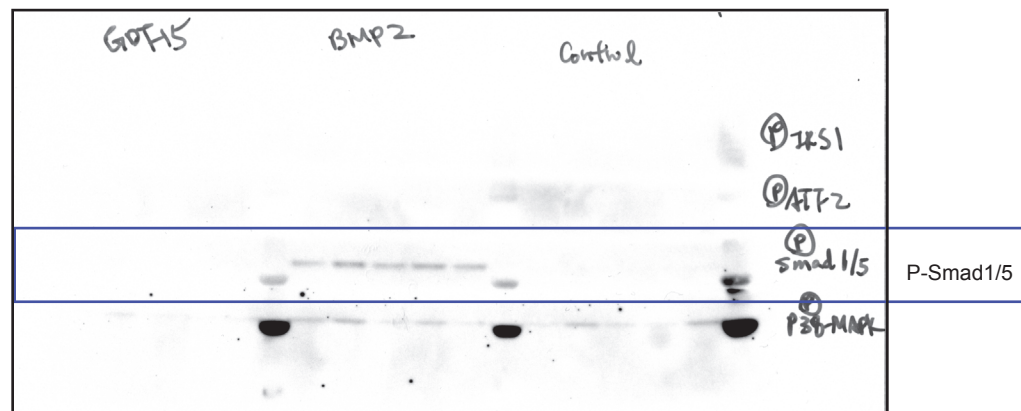
A



B



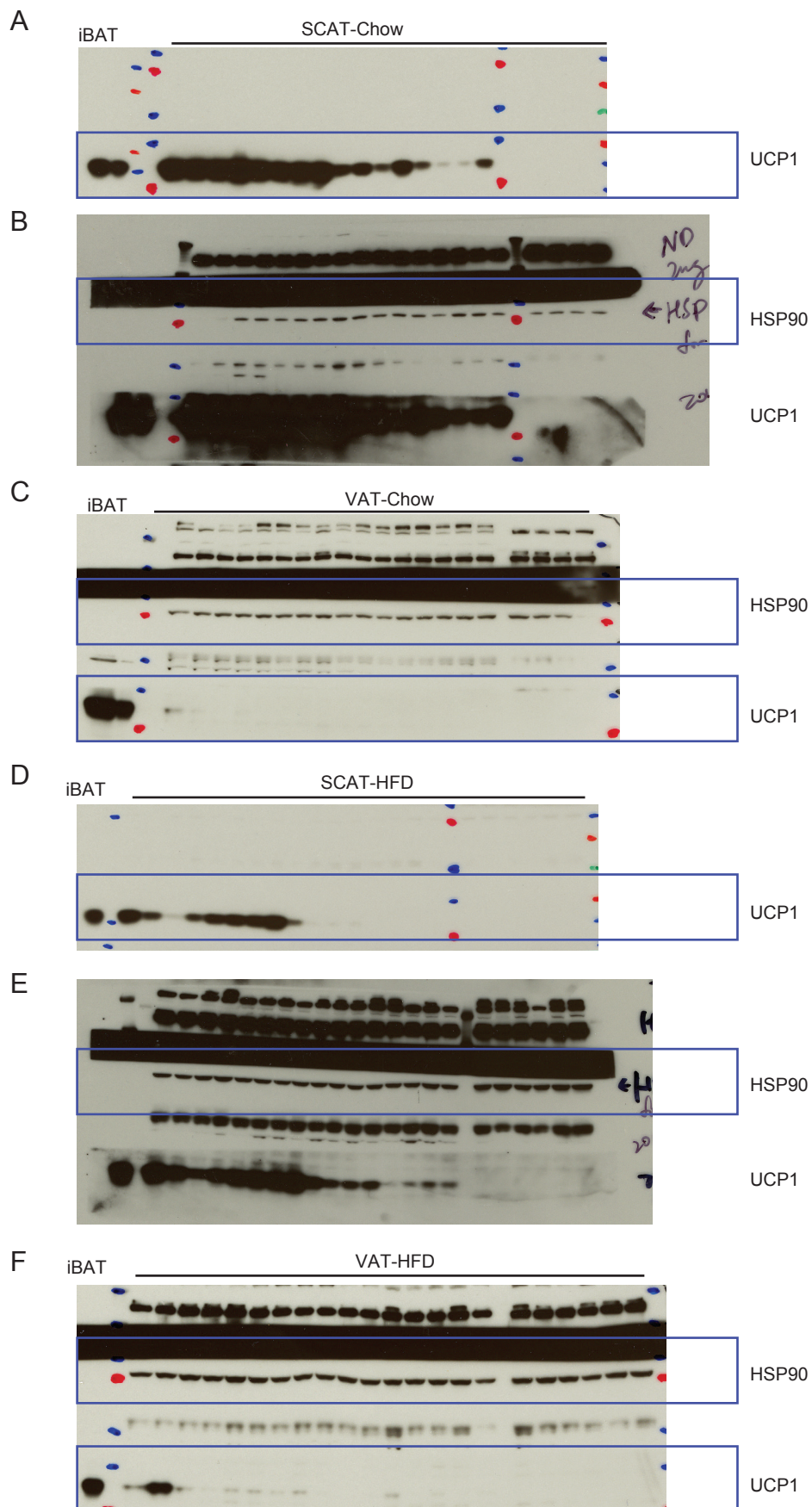
C



Supplemental Figure S6. Scanned raw images for the western blot images shown in Figure 5C.

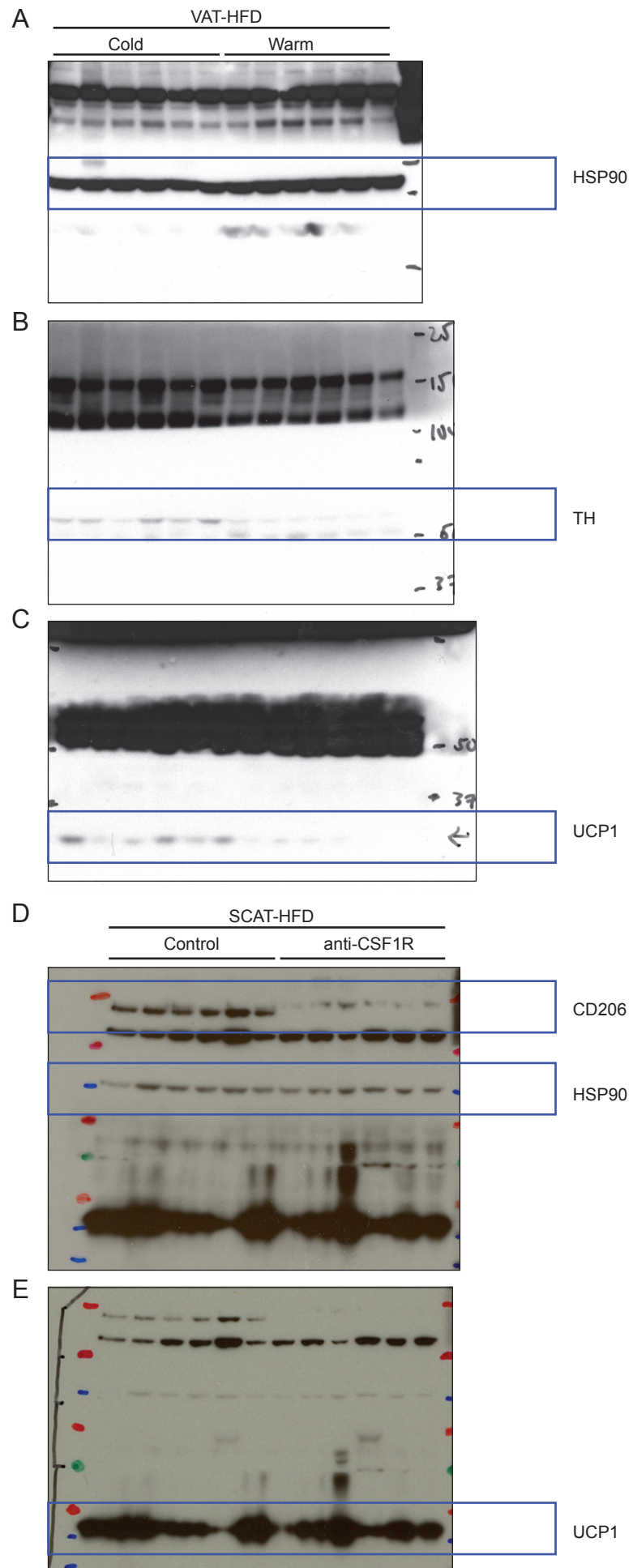
Nitrocellulose membranes were cut into stripes for different antibody staining. (A) and (B) are the same blot with different exposure time. (C) is a different blot from (A) and (B), but from a gel loaded with the same amount of proteins, with the same order, and ran on the same time in the same gel tank. Blue boxes indicate the cropped images shown in Figure 5C. In Figure 5C, the images are flipped horizontally to show control samples on the left.

Fig. S7



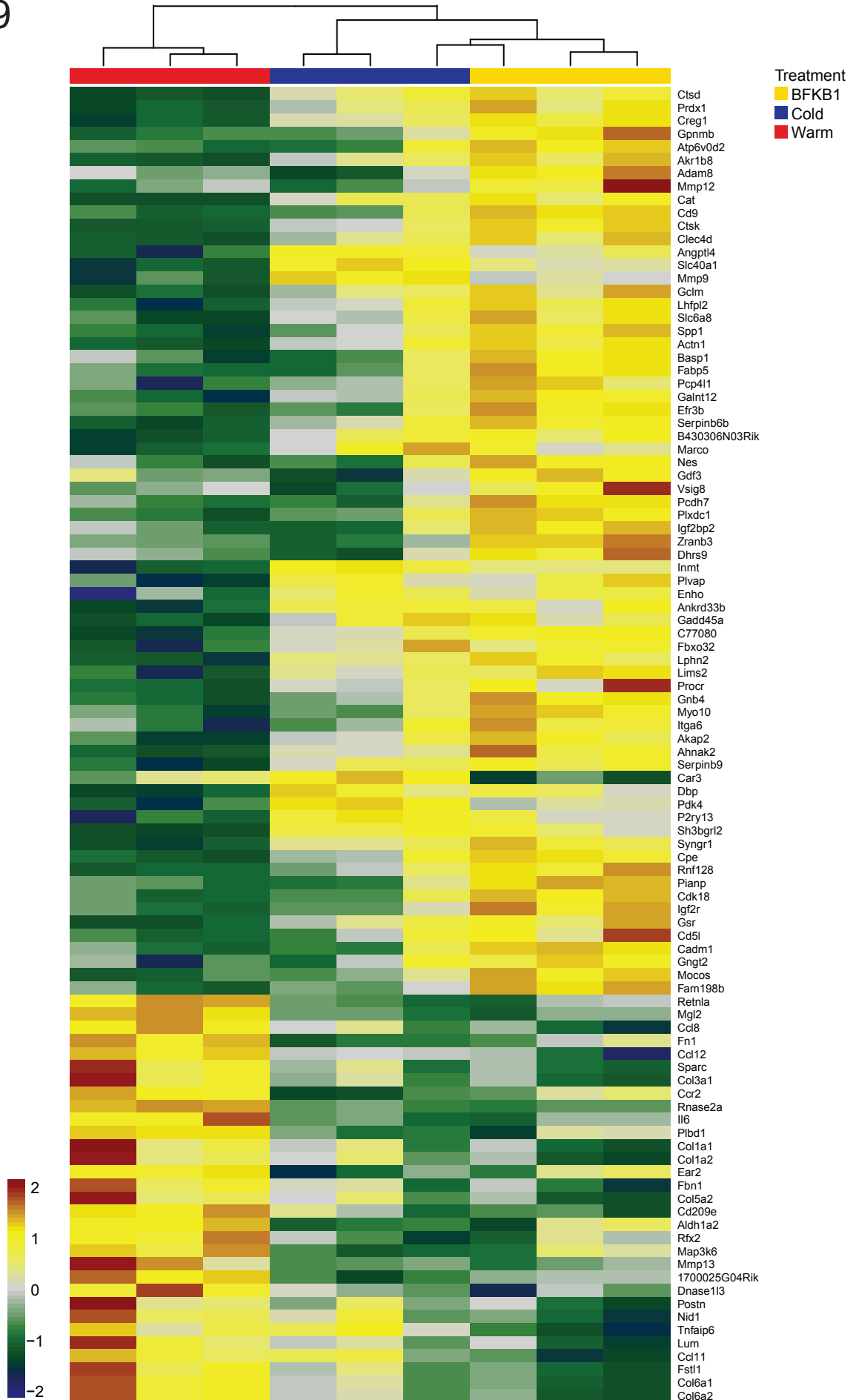
Supplemental Figure S7. Scanned raw images for the western blot images shown in Figure 1D and F. Nitrocellulose membranes were cut in stripes for different antibody staining. (A) and (B) are the same blots with different exposure time. (C) HSP90 and UCP1 expressions were shown in the same blot. (D) and (E) are the same blots with different exposure time. (F) HSP90 and UCP1 expressions were shown in the same blot. Blue boxes indicate the cropped images shown in Figure 1D and F. In Figure 1D and F, the images are flipped horizontally to show control samples on the left.

Fig. S8



Supplemental Figure S8. Scanned raw images for the western blot images shown in Figure 2I and Supplemental Figure S4H. Nitrocellulose membranes were cut in stripes for different antibody staining. (A) gel was processed and loaded the same amount of proteins as (B) and (C). (B) and (C) are the same blots with different exposure time. (A) HSP90, (B) TH, and (C) UCP1 expressions were shown. (D) and (E) are the same blots with different exposure time. (D) HSP90 and CD206, and (E) UCP1 expressions were shown in the same blot. Blue boxes indicate the cropped images shown in Figure 2I and Supplemental Figure S4H. In Figure 2I, the images are flipped horizontally to show control samples on the left.

Fig. S9



Supplemental Figure S9. Heatmap with gene names shown in Figure 6J.

Table 1. Reagent used for the study

REAGENT	SOURCE	IDENTIFIER
Antibodies and related reagents		
Anti-CD45 MicroBeads	Miltenyi Biotec	130-052-301
Anti-CD31 MicroBeads	Miltenyi Biotec	130-097-418
Purified Rat Anti-Mouse CD16/CD32 (Fc Block™)	BD Biosciences	553141
Anti-CD45	BioLegend	30-F11
Anti-CD31	BioLegend	390
Anti-Podoplanin	BioLegend	8.1.1
Anti-PDGFR α	BioLegend	AP5
Anti-Lyve1	BioLegend	ALY7
Anti-Lyve1	R&D Systems	223322
Anti-CD11c	BioLegend	N418
Anti-CD206	BioLegend	C068C2
Anti-Gr1	BioLegend	RB6-8C5
Anti-FceR1	BioLegend	MAR-1
Anti-Siglec-F	BDbiosciences	E50-2440
Anti-F4/80	BioLegend	BM8
Anti-CD11b	BioLegend	M1/70
Anti-CD29	BioLegend	HMb1-1
Anti-Sca-1	BioLegend	E13-161.7
Anti-Class III β -tubulin (Tubb3)	BioLegend	AA10
Anti-CD206	Abcam	ab64693
Anti-UCP1	Abcam	ab23841
Anti-TH	EMD Millipore	AB152
Anti-TH	EMD Millipore	MAB318
Anti-Smad1	Cell Signaling Technology	9743
Anti-Phospho-Smad1/5	Cell Signaling Technology	9516
Anti-mouse IgG HRP-linked	Cell Signaling Technology	7076
Anti-rabbit IgG HRP-linked	Cell Signaling Technology	7074
Anti-Lyve-1	R&D Systems	AF2125
Anti-CD206	R&D Systems	AF2535
Anti-F4/80	BioRad	MCA497G
Anti-Coll	Abcam	ab21286
Anti- α SMA	Sigma	c6198
Anti-Arg1	Abcam	ab60167
Anti-Arg1	Abcam	ab124917
Anti-TUBB3	Abcam	ab18207
Anti-Ret	Abcam	Ab134100
Anti-HSP90	Cell Signaling Technology	#4877
Anti-FGFR1/KLB bispecific antibody	Genentech	bFKB1
Anti-Ragweed (RW, isotype control)	Genentech	
Trastuzumab (Herceptin, isotype control)	Genentech	
Anti-mouse CSF1R	BioXCell	BE0213

isotype control Rat IgG2a	BioXCell	BE0089
Picro Sirius Red	Abcam	ab150681
DAPI	Thermo Scientific	62247
Hyaluronan binding protein (HABP)	EMD Millipore	#385911
Recombinant Proteins		
Recombinant human/mouse BMP2	R&D Systems	355-BM
Recombinant human GDNF	R&D Systems	212-GD
Recombinant human His-GDF15, CHO	Genentech	PUR121320
Recombinant human Fc-GDF15, HEK293T	Genentech	PUR125052
qPCR primers		
TBP_F: ATCAACATCTCAGCAACCCA TBP_R: TTGAAGCTGCGGTACAATTC	Genentech	N/A
Pparg1a_F: CCCTGCCATTGTTAAGACC Pparg1a_R: TGCTGCTGTTCCCTGTTTTTC	Genentech	N/A
Scd1_F: CTGTACGGGATCATACTGGTTC Scd1_R: GCCGTGCCTTGTAAGTTCTG	Genentech	N/A
Rpl13A_F: GAAGGCATCAACATTTCTGGAA Rpl13A_R: CAGTGCGCCAGAAAATGC	IDT	Mm.PT.58.43547045 .g
Tbp_F: TGTATCTACCGTGAATCTTGCC Tbp_R: CCAGAACTGAAAATCAACGCAG	IDT	Mm.PT.39a.2221483 9
Pparg1a_F: TGCAGCCAAGACTCTGTATG Pparg1a_R: TCAGAAAGGTCAAGTTCAGGAAG	IDT	Mm.PT.58.28716430
Ucp1_F: CAAATCAGCTTTGCCTCACTC Ucp1_R: CACACCTCCAGTCATTAAGCC	IDT	Mm.PT.58.7088262
Plasmid DNA		
pFA2-ELK1	Agilent	219062
pFR-luc	Agilent	219050
pRL-SV40	Promega	E2231
CMV-Human Ret51	Genentech	J4006
CMV-Human Gfral	Genentech	DNA751304
CMV-Human Gfra1	Genentech	DNA365770